New Renaissance Institute®
Technology White Paper (Preliminary)

A Frequency Comparator for Fixed and Modulated Waveforms Utilizing Enveloping-Event Detection: A Theoretical Background Employing a Symbolic Dynamics Framework

 Updated November 21, 2005

Abstract

Frequency and phase comparators are classic elements of signal processing circuits and algorithms. This whitepaper provides a theoretical background, employing a symbolic dynamics framework, for a novel approach to frequency and phase comparators for pairs of square or pulse waves of different frequencies that are not phase-locked. The theory and related technology have other applications. The approach, various implementations, and applications are patent pending.

As the relation between transitions in the two non-phase-locked pulse waveforms fluctuates over time, there will be intervals over which the wave of higher frequency will make two consecutive transitions between its higher and lower amplitudes, while the wave of lower frequency makes no such transition. This creates a symbolic signature that characterizes relative frequency and duty cycle relationships among the square wave signals. By detecting simple patterns in sequences of symbols generated in this way, it is possible to determine which waveform has the higher frequency. The approach, initially applied to the dynamics of symmetric pulse waves, is extended to explain the dynamics of asymmetric pulse waves.

Implementations are described in a companion whitepaper, and these have several advantages over existing approaches. Only original signals and signal feed-forward are involved, resulting in feedback-free implementations that operate over a very wide range, and do not require any input signal to be in quadrature form. Implementations may employ either state or transition analysis, may be event-driven or periodically sampled, and may be realized either in hardware or as algorithms. Implementations may be expanded to include more than two signal inputs and asymmetric pulse waveforms.

INTRODUCTION

Frequency and phase comparators are classic elements of electrical circuits. They are used in a wide variety of applications in communications, signal analysis and other areas. Many different approaches to implementing frequency and phase comparators have been proposed. Existing approaches include the use of digital counters, analog integrators, quadrature-phase signal formats provided in parallel, and state machines with state feedback.

This whitepaper describes the theoretical background for a novel approach to implementing frequency and phase detectors. In contrast to existing devices, devices based on this approach use only feed-forward state signal flows. This approach exploits a feature of pairs of square or pulse waves of different frequencies that are simultaneously generated: as the relation between the two waves fluctuates over time, there will be intervals over which a half-cycle of the wave of lower frequency will surround or "envelop" a half-cycle of the wave of higher frequency (provided the waves are not phase-locked). More precisely, during these intervals the wave of higher frequency will make two consecutive transitions between its higher and lower amplitudes while the wave of lower frequency has the same amplitude. Detecting these enveloping events provides a way to determine which wave has the higher frequency, as well as to obtain other information. The enveloping events may be detected by monitoring the pattern of states or state transitions associated with pairs of square waves.

This novel approach to determining which of two waves of different frequencies has the higher frequency provides the basis for at least two new classes of frequency comparators. In a first class of implementations, these square wave enveloping events are detected by identifying consecutive opposite transitions in one signal occurring between consecutive opposite transitions of the other signal.

In a second class of implementations, the instantaneous values of the two square waves are regarded as a symbol of asynchronous state. Square wave enveloping events are detected by identifying signature symmetries in the resulting sequence of symbols. Realizations of this second class of implementation amount to interpreting the relative values of the two applied square waves as a type of symbolic dynamics to which pattern detection is applied. This class of implementation can be used to provide additional detailed information, such as a course indication of relative phase. This can be done, for example, by utilizing specific symbol sequence signatures that can be detected in real time.

The remainder of this whitepaper discusses the theory behind this approach to implementing frequency comparators, utilizing a symbolic dynamics framework. (A companion whitepaper, "A Frequency Comparator for Fixed and Modulated Waveforms Utilizing Enveloping-Event Detection: Implementations and Applications," discusses circuit and algorithmic implementations of this approach.) The technologies described in this whitepaper are protected by a pending U.S. Patent and other affiliated patents licensable from New Renaissance Institute®. New Renaissance Institute® can provide detailed hardware and software reference designs under negotiable terms. All financial or in-kind proceeds from such arrangements are used to fund pure academic research at New Renaissance Institute®.

STATE VIEW OF THE DYNAMICS OF A SQUARE WAVE PAIR

At a high level, a state may be associated with pairs of square waves by treating the instantaneous measured value of the two square waves as a two-component vector. For example, a first square wave signal A and a second square wave signal B may each take on values of 0 or 1 at any particular time (ignoring noise and transition-related transient phenomena). There would be four resulting states, named by the symbols S_0, S_1, S_2 and S_3 in Table A:

Table A.

S_x	A	B
S_0 =	0	0
S_1 =	0	1
S_2 =	1	0
S_3 =	1	1

This symbol assignment is given by the formula:

$S_{(2a+b)}$

where "a" is the instantaneous value of A (either 0 or 1) and "b" is the instantaneous value of B.

The first square wave signal A and the second square wave signal B typically originate from an exogenous signal source and may be measured in asynchronous (effectively) continuous time or in synchronously-sampled discrete time. Each type of measurement creates a temporal sequence of the symbols S_0, S_1, S_2 and S_3.

Figure 1a shows the case for continuous-time measurement, which produces an "event-driven" sequence of symbols, while Figure 1b shows the case for synchronously-sampled discrete-time measurement, which produces a "time-driven" sequence of symbols. Referring to Figure 1a the graphs of a first square wave signal A and a second square wave signal B, each of which is allowed to take on one of two values at any given time, are shown evolving in time, with time increasing from left to right. The first square wave signal A is shown progressing through an "up" transition from a lower value to a higher value, followed later in time by a "down" transition from the higher value to the lower value. This is followed by additional subsequent "up" and "down" transitions. Similarly, the second square wave signal B is shown progressing through a "down" transition and an "up" transition, as well as additional subsequent transitions. Between each of the transitions, the pair of waveforms maintains a fixed state corresponding to one of the symbols S_0, S_1, S_2 and S_3, and the state changes to another symbol after the next transition. Thus, any transition in either of the two square wave signals A or B causes a state transition, or symbol transition, event, between which the state is constant. For example, in the figure, the state just prior to transition event a is S_1 (A=0, B=1), the state between transition event a and transition event b is S_0 (A=0, B=0), the state between transition event b and transition event c is S_2 (A=1, B=0), the state between transition event c and transition event d is S_3 (A=1, B=1), etc. The result is an "event-driven" sequence of symbols $\{S_1, S_0, S_2, S_3 \ldots\}$.

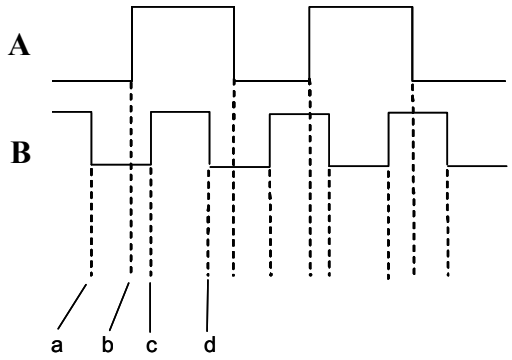

Figure 1a Event-driven

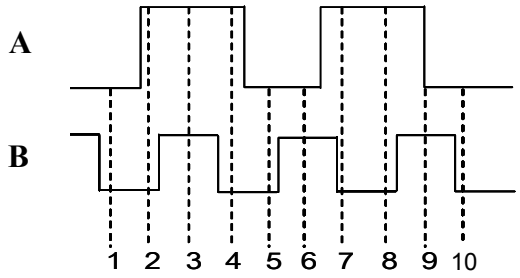

Figure 1b Time-driven

Figure 1b shows the case for synchronously-sampled discrete-time measurement, which produces a "time-driven" sequence of symbols. Here the values of the same first square wave signal A and the same second square wave signal B are periodically measured at sample times 1-10, and the value of a state measured at one sample time is maintained until the next sample time. Such an arrangement is useful in regular clock-driven signal processing implementations. In the example of Figure 1b, the state at sample time 1 is S_0, the state at sample time 2 is S_2, the state at sample time 3 is S_3, etc. Note that the state at the two consecutive sample times 7 and 8 is S_2. If the rate of sampling were considerably faster than that depicted, situations where the same state is held for consecutive sample times would happen frequently. By definition, the event-driven symbol sequence cannot have consecutively repeated symbols (as a driving "event" corresponds to the change in state, hence change in symbol). Thus, for the same pair of square waves, an "event-driven" sequence of symbols will typically differ from a "time-driven" sequence of symbols. Figures 1e-f show a comparison of the permissible state transitions among the states represented by symbols $\{S_0, S_1, S_2, S_3 \ldots\}$ for event-driven and time-driven measurements.

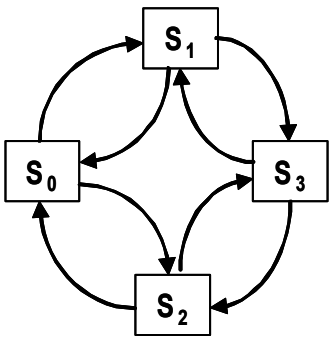

Figure 1c Event-driven

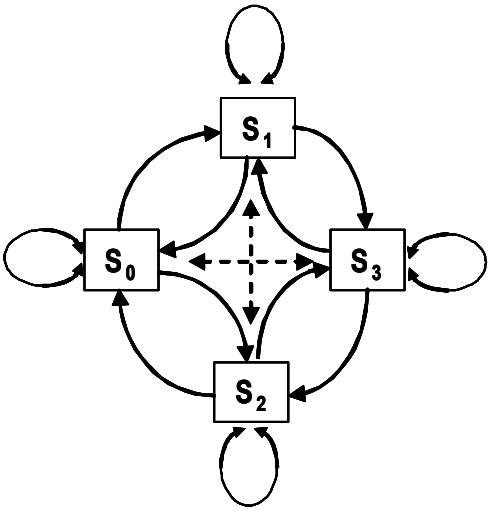

Figure 1d Time-driven

In the event-driven case of Figure 1e, direct transitions between symbol pairs S_0 and S_3 and between symbol pairs S_1 and S_2 are forbidden as either would require both square wave signals A and B to change states simultaneously, a physically improbable condition except in pathological cases, and even then overruled by circuitry race conditions. Also, in the event-driven case of Figure 1C, each state may transition only to another state, not back into itself. This is because, by definition, if there is no observed state transition there is no new event--hence no repeated event symbols are possible. Taken together, the forbidden state transitions are those where the current symbol and the immediately previous symbol are either equal (both square wave signals transition back to the same state) or complements of one another (both square wave signals A and B change states simultaneously).

In the time-driven case of Figure 1d, transitions from a state back into itself are not only possible, but dominate the time-driven symbol sequence as the sampling rate increases. It is clear, however, that if the sampling rate is high enough to capture the effect of every transition in each of the pair of square waves (i.e., the sampling rate is at least twice the frequency of the higher-frequency square wave), the resulting time-driven event sequence can be transformed into an approximate event-driven sequence (such as that of Figure 1a) where the only errors introduced are ones of time-quantization delays. This transformation may be done, for example, by omitting any repeated sample values. Additionally, in the time-driven case of Figure 1d, direct transitions between symbol pairs S_0 and S_3 and between symbol pairs S_1 and S_2 are in some circumstances possible, for example:

- if the sampling rate is slow enough (the faster the sampling rate, the less likely this situation will occur);
- if the square wave signals A and B are digitally generated, of frequencies that are ratios of integers, and phase-locked.

These sampling-rate artifact transitions are indicated by the dotted lines in Figure 1d. Care must be taken to adequately and stably handle cases where the sample time effectively coincides with a transition in one of the waveforms, as with sample time 9 in Figure 1b.

Whether obtained directly as in Figure 1a or derived from a time-driven symbol sequence, the measurements of the two square waves ultimately provide an actual or approximate event-driven symbol sequence. The measurements themselves may be made on the sustained values of the square wave, as called out by the bolded portions of the square wave in Figure 1e, or may be made on the transitions of the square wave, as called out by the bolded arrows of the square wave in Figure 1f.

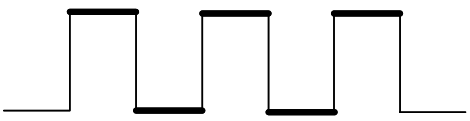

Figure 1e State-determined

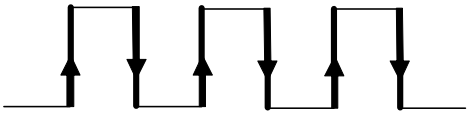

Figure 1f Transition-determined

ENVELOPING EVENT PHENOMENA

With these concepts in place, the "enveloping-event" phenomena peculiar to square waves of different frequencies can now be described. Figure 2a shows again a first square wave signal A, which has a lower frequency and thus a longer, wider-spread period than a second square wave signal B. In the figure, there are two special events, labeled "Enveloping Event 1" and "Enveloping Event 2," where signal B makes both an up transition and a down transition during an interval where signal A is unchanged. On either side of these transitions in signal B, signal A makes an up transition and down transition. In this sense, an up-down or down-up "pulse" of signal B is enveloped by an up-down or down-up "pulse" of signal A, and this can clearly only occur if the frequency of B is higher than the frequency of A. If the frequency of signal B is sufficiently higher than depicted in Figure 2a, even more transitions of signal B would be enveloped within an up-down or down-up "pulse" of signal A. An example of this can be found in Figure 2b, where several transitions of the square wave signal A_2 are enveloped by an up-down "pulse" of the square wave signal B. Thus, a sufficient condition for a first square wave to have a lower frequency than a second square wave is for there to be at least one consecutive pair of "up" and "down" transitions of the second square wave between a consecutive pair of "up" and "down" transitions of the first square wave. This condition will be referred to as an "enveloping event." There are eight types of enveloping events, which will be discussed in conjunction with Figure 2c after four additional important remarks.

- First, although an enveloping event is sufficient for one square wave to be determined as having a higher or lower frequency than another, it is not a necessary condition. For example, if two square waves of different frequencies are phase-locked, there are many classes of conditions where enveloping events cannot occur. Similarly, if the two square waves are sufficiently close in frequency (for example, originating from two cesium clocks), the two square waves are effectively phase-locked for the probable application interval (or lifetime) of the system. However, in many applications the two square waves are from separate sources and conditions that are not phase-locked and at frequencies sufficiently different so that enveloping events naturally and regularly occur. Further, in phase-locked applications, enveloping events can be selectively created or prevented by means of frequency-shift and phase-shift modulation for use in communications systems.
- Second, enveloping events can be detectable over a wide range of frequencies. The limiting case is where the frequencies of two square waves are very close. Referring to Figure 2b, if the frequencies of the two square waves A_1 and B are very close, the detection arrangement must be able to resolve narrow widths (the regions between the arrows) of the enveloping of wave B by wave A_1. Also, more frequently than not the widths of enveloping will be asymmetric and at times considerably so, thus requiring even higher performance in resolving narrow widths of enveloping.

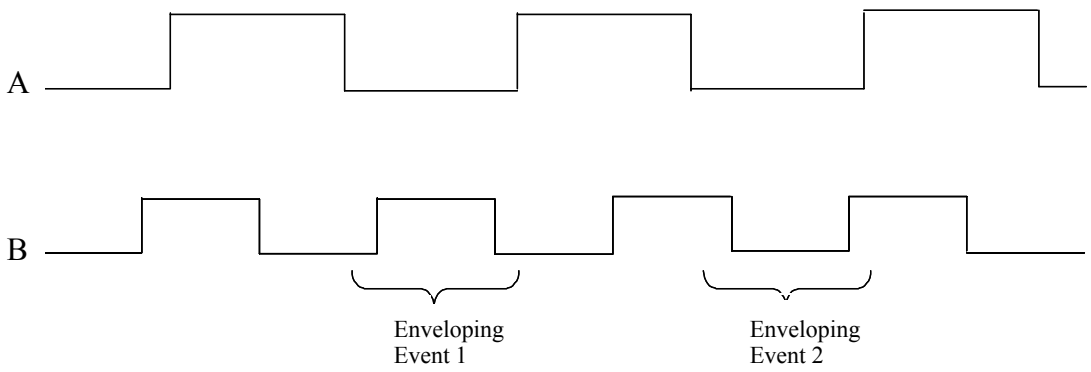

Figure 2a

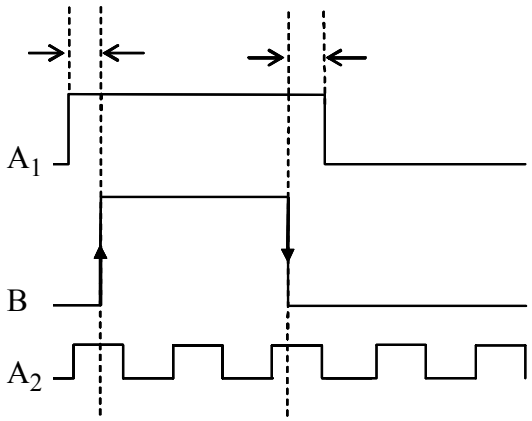

Figure 2b

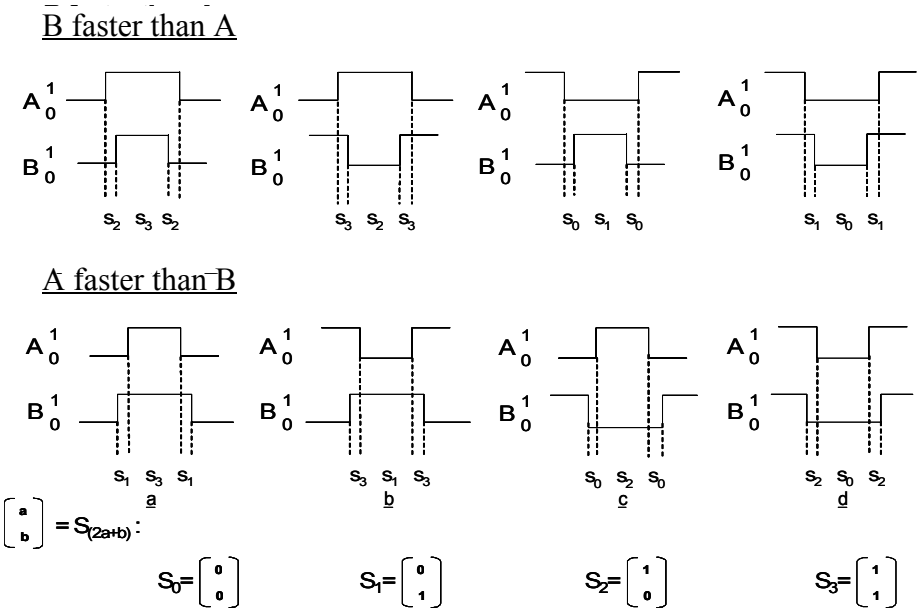

Figure 2c

- Third, to achieve the full range of operation, the arrangement for detecting enveloping events must strictly determine that both square waves have separately completed their consecutive pair of "up" and "down" transitions. Simply detecting that a first square wave has had a consecutive pair of "up" and "down" transitions with the value of a second square wave having the same value, as might be attempted in simple implementations involving edge-triggered D flip flops, will give at least some false results. As an example of such false results, note that both square waves A_1 and A_2 have the same value on the square wave B up transition as they do on the subsequent square wave B down transition. However, it is clear that the frequency of square wave A_1 is less than the frequency of square wave B, while the frequency of square wave A_2 is greater than the frequency of square wave B.
- Fourth, it is noted that the approach of the invention described thus far can be sensitive to square wave asymmetry. At least some enveloping event conditions can be violated if pulse widths are not 50%, and enveloping events can be falsely generated if duty cycles are extreme with respect to the difference in periods of the two waveforms.

Finally, note that if a first square wave has a lower frequency than a second square wave, the transitions of the second square wave happen at a faster rate than the transitions of the first square wave. In subsequent discussions this is a useful dominating concept, so the label "X faster than Y" will be useful as a name for the condition where the frequency of a square wave X is higher than the frequency of a square wave Y.

ENVELOPING EVENTS AS SYMMETRY EVENTS IN CONSECUTIVE STATES AND SOME OF THEIR PROPERTIES

Referring to Fig 2c, it may be seen that there are eight types of enveloping events. Enveloping may be with either of the square waves having a given or opposite polarity, giving four types of events. Either square wave may be the "faster" (higher frequency) one, giving two cases for these four types, or eight cases altogether. It is useful to characterize the cases using the state symbols S_0, S_1, S_2 and S_3 introduced earlier. The result is the following:

- Cases where B is faster than A:
  - $S_2\, S_3\, S_2$
  - $S_3\, S_2\, S_3$
  - $S_0\, S_1\, S_0$
  - $S_1\, S_0\, S_1$
- Cases where A is faster than B:
  - $S_1\, S_3\, S_1$
  - $S_3\, S_1\, S_3$

- $S_0\, S_2\, S_0$
- $S_2\, S_0\, S_2$

Thus the "signature" of one square wave having a faster rate (higher frequency) than another, is the existence of "symmetry events" of the form

$S_p\, S_q\, S_p$

as it is impossible for two square waves of the same frequency to have these symmetric symbol sequences.

Figure 3a summarizes the findings of Figure 2c in a state-oriented form, rearranging the ordering to index the outer symbols in ascending order. The state is also indicated in vector form, representing separate samples, 2-bit words in a shift register, etc. The findings of Figure 2c may alternatively be represented in a transition-oriented form, indicating which square wave has enveloping transitions, in which order these transitions occur, and what value the other square wave maintains throughout the enveloping event. Further, it is useful to more concisely name each of the eight symmetry events with a "symmetry event symbol" using the following notation:

$w_{pq} = S_p\, S_q\, S_p$

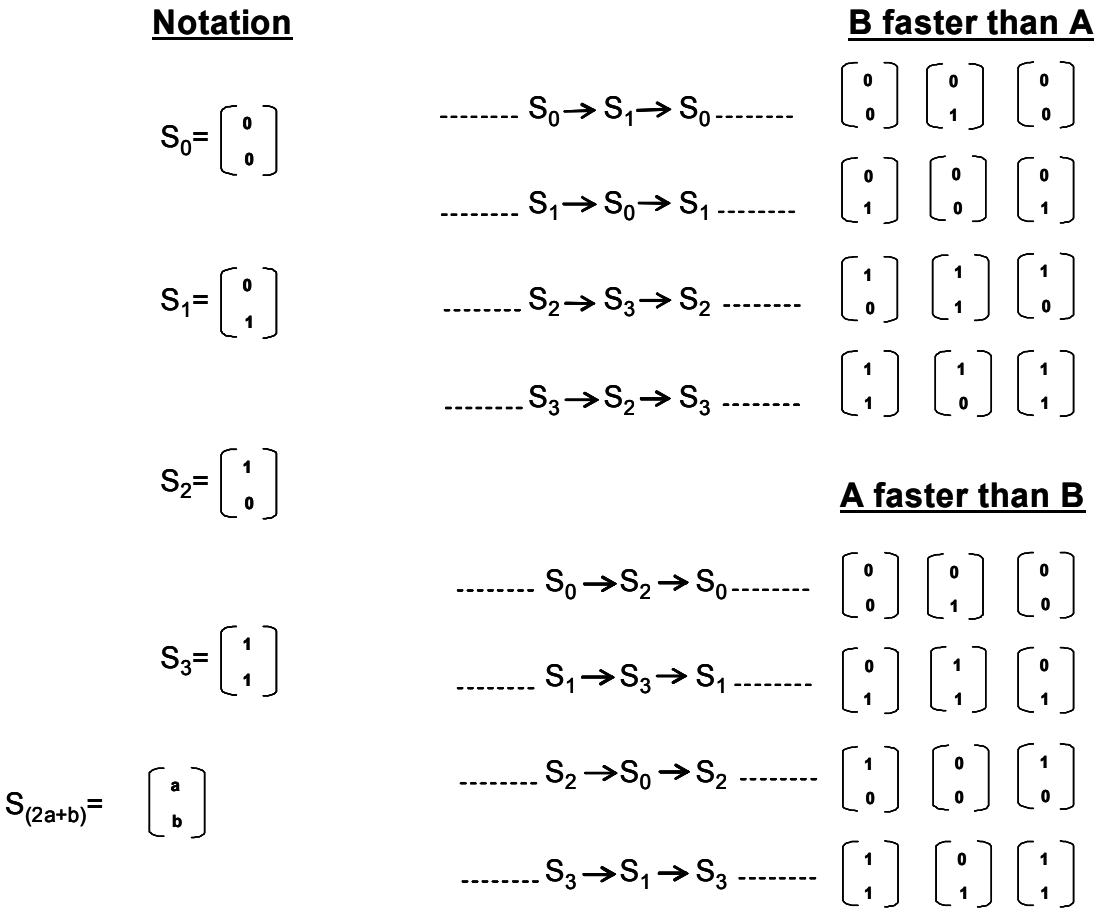

Figure 3a

Symmetric-Event Symbol	Symbol Sequence	Waveform View	Transition Representation	Higher Freq
W_{01}	s_0 s_1 s_0	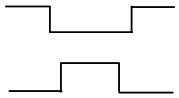	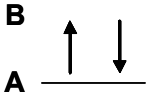	B
W_{10}	s_1 s_0 s_1	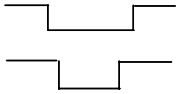	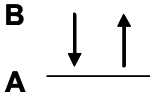	B
W_{23}	s_2 s_3 s_2	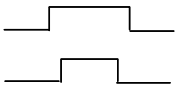	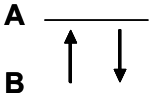	B
W_{32}	s_3 s_2 s_3	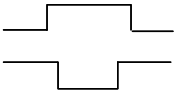	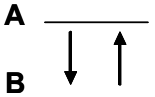	B
W_{02}	s_0 s_2 s_0	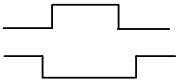	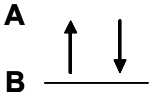	A
W_{13}	s_1 s_3 s_1	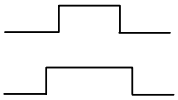	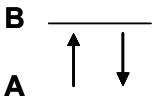	A
W_{20}	s_2 s_0 s_2	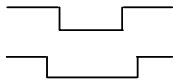	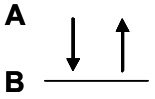	A
W_{31}	s_3 s_1 s_3	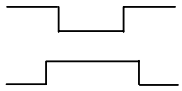	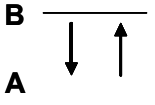	A

Figure 3b

Figure 3b consolidates this notation, the results of Figure 3a, and a representation of transition-oriented forms into a single table. The representation of transition-oriented forms is rendered according to the following rules:

- The faster square wave is represented with a pair of arrows reflecting consecutive transitions in its signal amplitude in the enveloping event.
- The slower square wave is represented with a horizontal line. This horizontal line is drawn above the pair of transition arrows if the slower square wave maintains a high value throughout the transition event, and is drawn below the pair of transition arrows if the slower square wave maintains a low value throughout the transition event.

- The source of each square wave (i.e., A or B) is written to the left of its representation.

Inspection of Figure 3b shows there are a number of striking structural relationships exhibited, suggestive of possible underlying permutation group phenomena and worthy of further study. Figure 4 draws attention to two particular views of the structural relationships and reveals yet more, perhaps unexpected, structure. The left table is organized with the common center symbol indexed in increasing order, and lists the rate-distinguishing outer symbols, which indicate which of the two waves is faster. The right table is organized exactly oppositely, with the outer symbols indexed in increasing order, and lists the rate-distinguishing common center symbol, which indicates which of the two waves is faster. In fact, the two tables have exactly the same entries. Further, the two rate-distinguishing columns in both tables are, reading from top to bottom, in retrograde (i.e., of opposite order).

Common Center Symbol	Rate-Distinguishing Outer Symbols	
	A faster than B	B faster than A
S_0	S_2	S_1
S_1	S_3	S_0
S_2	S_0	S_3
S_3	S_1	S_2

Common Outer Symbol	Rate-Distinguishing Inner Symbols	
	A faster than B	B faster than A
S_0	S_2	S_1
S_1	S_3	S_0
S_2	S_0	S_3
S_3	S_1	S_2

Figure 4

Some further structural analysis will be useful. First, exclusive pairings are noted in the formation of symmetry events:

- For B faster than A:
  - S_0 is always paired with S_1
  - S_2 is always paired with S_3
- For A faster than B:
  - S_0 is always paired with S_2
  - S_1 is always paired with S_3

Next, in each of the frequency comparison cases “B faster than A” and “A faster than B,” each of the symmetry events has a unique “complement” (i.e., all 0’s and 1’s exchanged) within the same frequency comparison case:

- For B faster than A:
  - $w_{01} = w_{32}^*$

- $w_{10} = w_{23}^*$
- $w_{23} = w_{10}^*$
- $w_{32} = w_{01}^*$

- For A faster than B:
  - $w_{02} = w_{31}^*$
  - $w_{13} = w_{20}^*$
  - $w_{20} = w_{13}^*$
  - $w_{31} = w_{02}^*$

This is simply due to the fact that enveloping events occur with either polarity. Note in all cases that:

$w_{pq} = w_{(3-p)(3-q)}^*$

in part due to the way the symbols $\{S_0, S_1, S_2, S_3 \ldots\}$ have been indexed by the formula

$S_{(2a+b)}$

In a state-oriented implementation, the sequence of measured symbols may be examined for the occurrence of the eight possible symmetry event symbols so as to determine which square wave signal is faster. In an event-driven implementation, a symmetry event may be detected by comparing the current symbol value to the symbol value two events in the past: if they are identical, a symmetry event has just occurred. Once a symmetry event has been detected, it may be classified as a particular one of the eight possible symmetry event symbols based on the values of the current and immediately preceding symbols, following from the definitions of the symmetry event symbols w_{pq}, as shown in the following table

:

$S_{current}$		$S_{previous}$		**Symmetry-Event symbol**	**Frequency Relationship**
A	**B**	**A**	**B**		
0	0	0	0		
0	0	0	1	$\mathbf{w_{01}}$	**B** faster than **A**
0	0	1	0	$\mathbf{w_{02}}$	**A** faster than **B**
0	0	1	1		
0	1	0	0	$\mathbf{w_{10}}$	**B** faster than **A**
0	1	0	1		
0	1	1	0		
0	1	1	1	$\mathbf{w_{13}}$	**A** faster than **B**
1	0	0	0	$\mathbf{w_{20}}$	**A** faster than **B**
1	0	0	1		
1	0	1	0		
1	0	1	1	$\mathbf{w_{23}}$	**B** faster than **A**
1	1	0	0		
1	1	0	1	$\mathbf{w_{31}}$	**A** faster than **B**

1	1	1	0	w_{32}	**B** faster than **A**
1	1	1	1		

Reorganization of columns (by partitioning each symbol into its A and B components and putting like components in adjacent columns) yields a periodic clustering:

$S_{current}$	$S_{previous}$	$S_{current}$	$S_{previous}$	Symmetry-Event symbol	Frequency Relationship
A	**A**	**B**	**B**		
0	0	0	0		
0	0	0	1	w_{01}	**B** faster than **A**
0	0	1	0	w_{10}	**B** faster than **A**
0	0	1	1		
0	1	0	0	w_{02}	**A** faster than **B**
0	1	0	1		
0	1	1	0		
0	1	1	1	w_{13}	**A** faster than **B**
1	0	0	0	w_{20}	**A** faster than **B**
1	0	0	1		
1	0	1	0		
1	0	1	1	w_{31}	**A** faster than **B**
1	1	0	0		
1	1	0	1	w_{23}	**B** faster than **A**
1	1	1	0	w_{32}	**B** faster than **A**
1	1	1	1		

Additional theory can be developed for these and further structural observations, e.g.,

- further algebraic relationships,
- topological and geometric representations,
- connections to formal established symbolic dynamics theory,
- other phenomena with unique sequence phrase "signatures."

VIEW OF SQUARE WAVE PAIR DYNAMICS AS SYMBOLIC DYNAMICS

Symbolic dynamics, also known as topological dynamics, is a rich area of nonlinear science. The present invention provides for symbolic dynamics [1-6] interpretations of the dynamics of pairs of square waves. Such interpretations may be used as a design tool, or as a means for creating additional applications or extending functionality. In fact, the symbolic dynamics framework is an excellent setting in which to define and explain many aspects of the invention. Only a very small amount of the symbolic dynamics formalism, and practi-

cally none of the extensive theory, is necessary to obtain a useful engineering framework. This section presents the relevant material.

Figure 5 shows one general setting in which to think of a symbolic dynamics system [6 (page 1)], although many others, often far more mathematically abstract, are commonly used [3-6]. In one version, a continuous-valued time, continuous-valued state dynamical system has its states quantized, mapped to equivalence classes of states, projected onto a smaller collection of states, etc. All of these result in a small collection of discrete states (called symbols) which are arranged in a (discrete-time) sequence. The result is a mapping of the continuous-valued time, continuous-valued state dynamical system to a discrete-valued time, discrete-valued state (a.k.a. symbols) dynamical system. Equivalent discrete-valued time, discrete-valued state dynamical systems may model computers, machines, natural phenomena, etc., as well as equivalent abstract discrete-valued time, discrete-valued state dynamical systems that are purely mathematical. At a common level of abstraction, all of the equivalent forms may be thought of as identical. The study of the dynamics and other properties of such discrete-valued time, discrete-valued state dynamical systems is the subject of symbolic dynamics.

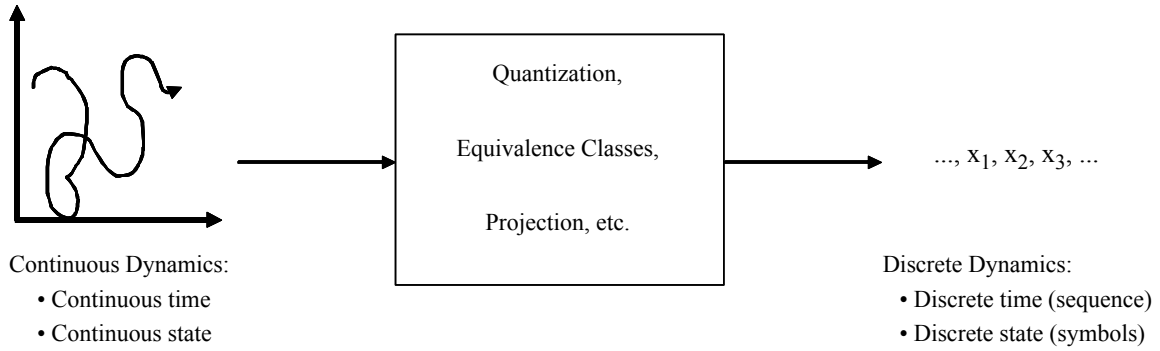

Figure 5

For the purposes of studying pairs of oscillators, some of the modeling machinery of symbolic dynamics is helpful. Figures 6a-c illustrate a torus model for the state-space of two continuous-valued oscillators. Here the periodic oscillations of one oscillator are represented as periodic motion in a vertical circle, while the periodic oscillations of the second oscillator are represented as periodic motion in a horizontal circle. As shown in Figure 6a, the combinations of the circular patterns sweep out the donut/bagel shape of a torus. If one associates the timekeeping within each period of each oscillator with a point moving in a circle and keeps track of this moving point for the combined pair of oscillators, the center of one circle is located along the circumference of the other circle in Figure 6a in a manner similar to adding the components of orthogonal vectors. This is illustrated in Figure 6b. As the points of each oscillator actually move, a trajectory is traced out along the surface of the torus as illustrated in Figure 6c. If one of the oscillators is faster than the other, it will wrap around the surface of the torus faster in its rotation direction than the other oscillator will wrap around the surface in its rotation direction. Note that all that is needed of the torus is its surface, and its interior is, for present purposes, hollow. In more formal terms, this torus

surface represents a continuous-valued state, continuous-valued time dual oscillator manifold, often used to describe or study uncoupled and coupled linear and nonlinear differential equations and other systems.

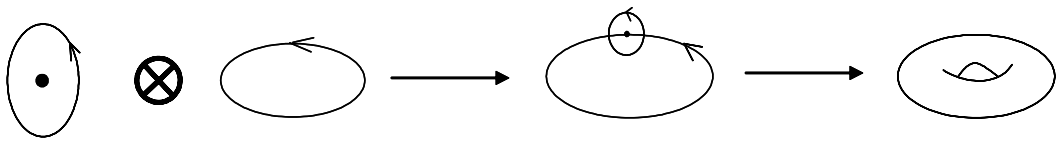

Figure 6a

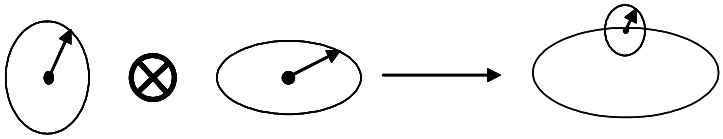

Figure 6b

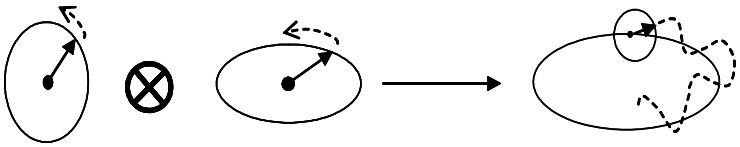

Figure 6c

In another view, a hollow torus may be cut once in each of the two orthogonal directions and flattened out. Figure 7a illustrates this. The flattened torus surface now has four edges resulting from the two cuts. If edge A' is rejoined or abstractly identified with edge A, to form a tube, and edge B' is rejoined or abstractly identified with edge B, to join the ends of the tube, the torus can be readily reconstructed. If both oscillators oscillated at precisely the same frequency, the composite state trajectory, if it started in the lower left corner of the flattened torus, would move along a diagonal line over time up to the far opposite corner. This traces out a connected winding path around the torus comprising exactly one wrap in each direction. This is depicted in Figure 7b. As time continues past the duration of one period, the curve repeats, and on the flattened torus, corresponds to starting over again at the original corner mentioned above. If the two oscillators oscillate at different frequencies, more complicated windings occur. For example, if the oscillator corresponding to the horizontal direction oscillates at twice the frequency of the oscillator corresponding to the vertical direction, the torus will be wrapped with two turns in one direction and one turn in the other direction. The corresponding paths on the flattened torus appear as shown in Figure 7c. Similarly, if the oscillator corresponding to the horizontal direction oscillates at three times the frequency of the oscillator corresponding to the vertical direction, the torus will be wrapped with two turns in one direction and one turn in the other direction; the corresponding paths on the flattened torus appear as shown in Figure 7d. The various copies of the flattened torus surface depicted in Figures 7c-d may be lined up side-by-side, like flooring or wall tiles, and the trajectory can be connected to form an uninterrupted path. This

"tiled" representation may be thought of as an unwrapped version of the wrapped trajectories on the surface of the unflattened torus.

The trajectories depicted in Figures 7b-d show cases where the ratio of frequencies is exactly the ratio of two integers. This causes the trajectory to eventually meet back where it started from, and repeat the pattern. The number of cycles involved for the repeat involves the least common multiple of the two frequencies. (More formally, the trajectories depicted in the examples of Figures 7b-d correspond to oscillator trajectories on manifolds for phase-locked, rational-valued frequency ratios of the two oscillators.) In cases where the ratio of frequencies cannot be expressed as a ratio of integers (i.e., as a rational number), the trajectory path on the torus never crosses itself. Additionally, Figures 7c-d illustrate how different integer frequency ratios between the two oscillators of Figures 6a-c result in differing wrapping characteristics and trajectory slopes

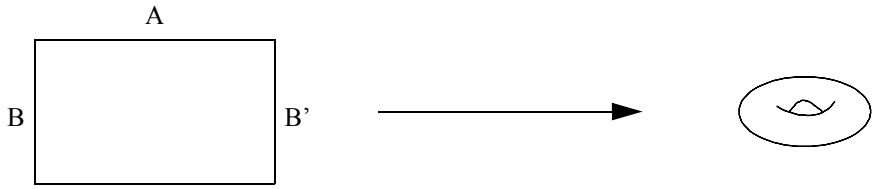

Figure 7a

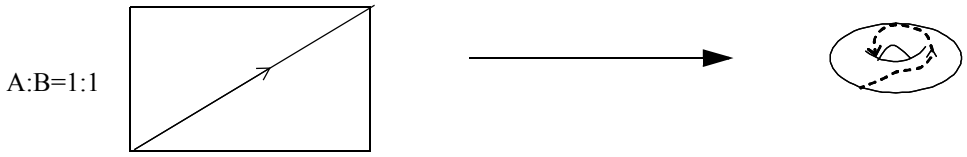

Figure 7b

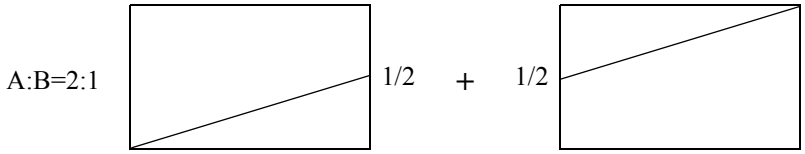

Figure 7c

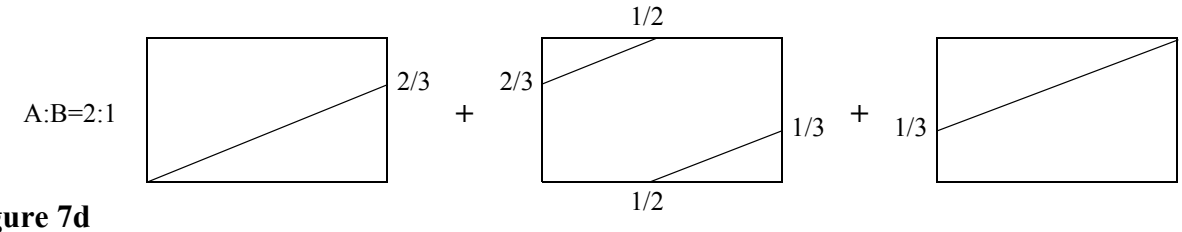

Figure 7d

This arrangement for abstracting the dynamic behavior of pairs of square waves can, in this way, be related to models of a dynamical system that, as a function of frequency ratio, produces either:

- a regular ("self organizing") pattern for so-called "commensurate" frequencies (i.e., the frequency ratio is a rational number), or
- an irregular pattern (i.e., "quasi-periodic" or "chaotic" behavior) for "incommensurate" frequencies (i.e., the frequency ratio is not a rational number).

Pairs of waveforms generated by asymmetric pulses, and pairs of waveforms whose frequencies are very close together, or whose frequencies are related to such frequencies by aliasing phenomena, exhibit very interesting and complex behavior. Nevertheless, they can be sufficiently well characterized to allow informative measurements with simple circuitry or algorithms like those that were described above, and like others that will be described below.

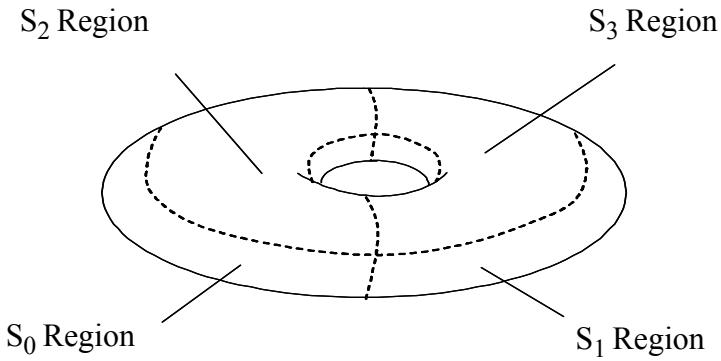

Figure 8

Figure 8 illustrates how the torus of Figures 6a-c and 7a-b may be symmetrically quantized into regions associated with the symbols employed by the invention. In particular, the symmetric quantization corresponding to the case where the input signals are symmetric square waves is depicted. The square wave model is naturally obtained by quantizing the continuous-valued continuous-time oscillator torus manifold into four regions corresponding to the symbols $\{S_0, S_1, S_2, S_3\}$ as shown in Figure 8. Portions of trajectory paths on the torus surface (manifold) may then be characterized according to which of the quantized sections they lie in, each corresponding to one of the symbols $\{S_0, S_1, S_2, S_3\}$. Referring to the left side of the torus of Figure 8, oscillations occurring only in horizontally-oriented loops (corresponding to, for example, oscillator A) alternate between symbols S_0 and S_2 while oscillations occurring only in horizontally-oriented loops on the right side of the torus alternate between symbols S_1 and S_3. Similarly, oscillations occurring in vertically oriented loops (corresponding to, for example, oscillator B) alternate between symbols S_0 and S_1 in the lower portion of the torus and between symbols S_2 and S_3 in the upper portion of the torus. With both oscillators A and B active, the trajectories may then cross through all four sections generating an event-driven symbol sequence comprising the symbols $\{S_0, S_1, S_2, S_3\}$. As a trajectory progresses from section to section, it may be thought of as generating an event-driven symbol sequence comprising the symbols $\{S_0, S_1, S_2, S_3\}$. In this way, the

present invention can be viewed in the more formal symbolic dynamics context. This model will be termed the "quantized-symbol torus model."

With this quantized-symbol torus model established, a corresponding infinite periodic symbol tiling model is next developed.

In Figures 7a-b the surface of the torus was represented as a flattened tile with edges that are identified together, so that a trajectory crossing a location of one edge reappears at the corresponding spot on the directly opposite edge. In Figures 7c-d, a trajectory passing over the surface of the torus in different ways was represented on a sequence of tiles. A general way to study complex wrappings of trajectories on the surface of the torus is to use a "tiling," where a sequence of adjacent images of tiles, each corresponding to a full copy of the surface of the torus, are arrayed edge-to-edge in a mosaic or grid.

In Figures 7b-c, trajectories relating to oscillations with a fixed frequency ratio appear as straight lines on each tile. The edge A' was joined with edge A of the same square and edge B' was joined with edge B of the same square to form the torus. Alternatively, each edge A' of a particular square may be identified with an edge A of a different neighboring square to the right, and each edge B' of a particular square may be identified with an edge B of a different neighboring square above. This forms a tiling--more precisely, an infinite periodic tiling. Neighboring tiles may extend without bound in both vertical and horizontal directions, and trajectories relating to oscillations with a fixed frequency ratio appear as straight lines over the sequence of tiles.

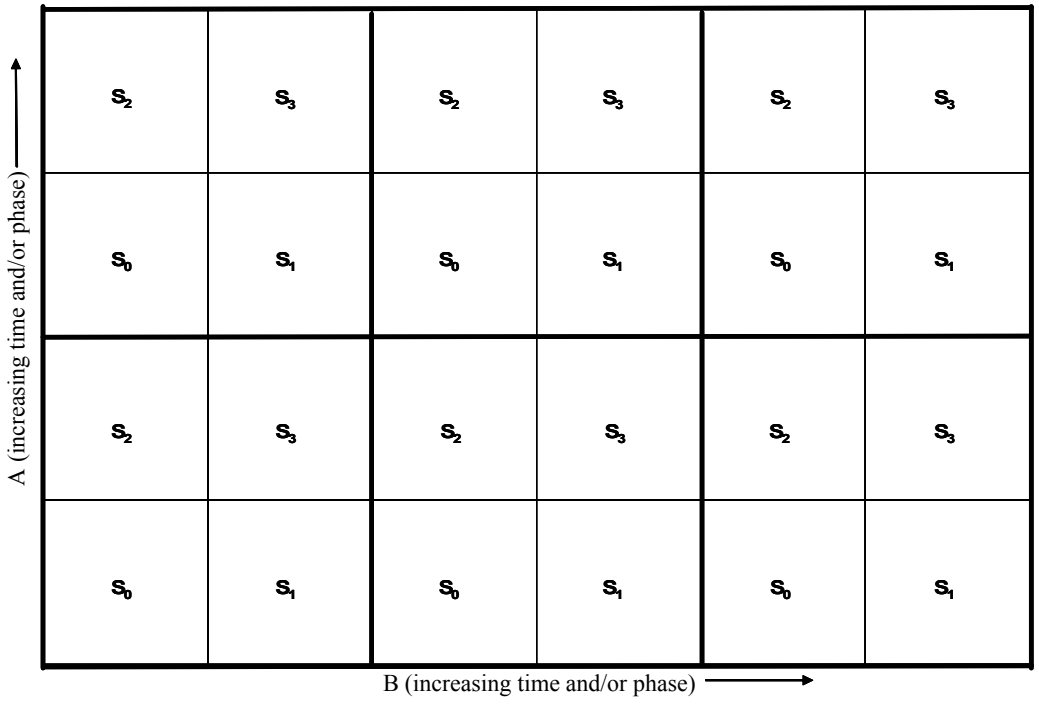

Figure 9a

Such an infinite periodic tiling may be further adapted to include the four regions of the symmetrically quantized torus of Figure 8. Figure 9a illustrates a sequential tiling representation of the symmetrically quantized torus of Figure 8. In this representation, motion in the vertical direction represents time or phase (or both) of one oscillator, and motion in the horizontal direction represents time or phase (or both) of the other oscillator. Each tile of the full torus surface is indicated with a thick line boundary and is evenly subdivided into four separate areas. These subdivided areas within each of the full torus-surface tiles will be termed "symbol tiles." In the vertical direction, there are two alternating types of columns, one that sequences between S_0 and S_2 symbol tiles and another that sequences between S_1 and S_3 symbol tiles. In the horizontal direction, there are two alternating types of rows, one that sequences between S_0 and S_1 symbol tiles and another that sequences between S_2 and S_3 symbol tiles. This model will be termed the "infinite periodic quantized-symbol tiling model." In this model, the arc-length of the trajectory corresponds linearly to measured time. Thus, for a trajectory with a slope of 2, oscillator A changes symbol tiles twice as fast as oscillator B.

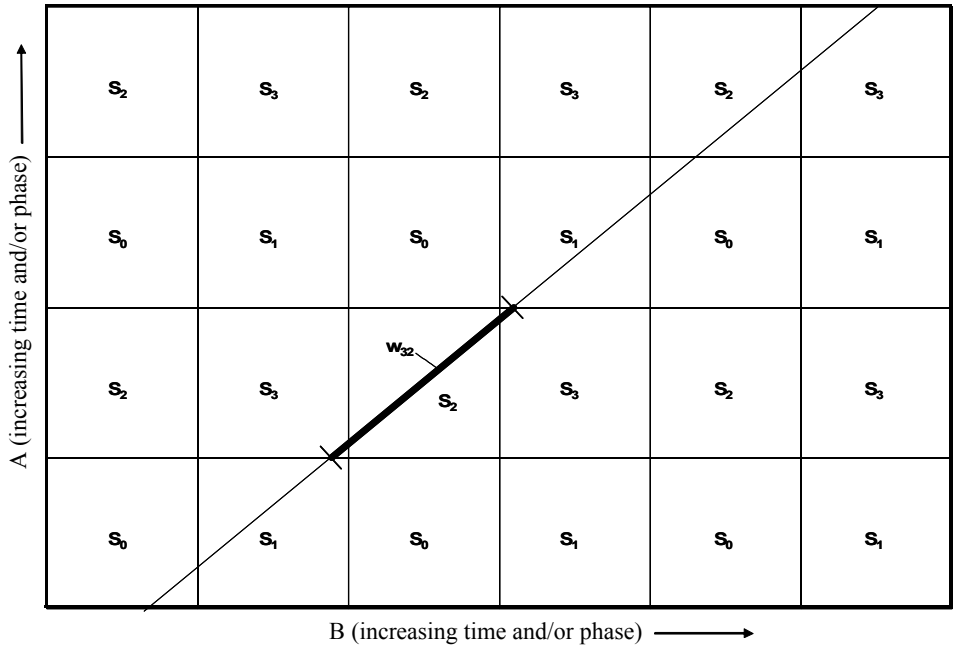

Figure 9b

When oscillators A and B are both active, the trajectories in this model may cross through any of the symbol tiles, and in this fashion may be seen as generating an event-driven symbol sequence comprising the symbols $\{S_0, S_1, S_2, S_3\}$ corresponding to those generated as a trajectory wraps around the torus. Figure 9b illustrates one possible trajectory on the sequential tiling representation of Figure 9a. For visual simplification, the thicker boundaries have been eliminated so that all boundaries are symbol tile boundaries. If the trajectory slope is not unity and the ratio of frequencies is not that of two integers, symmetry events will occur in the sequence of crossings of symbol tiles. Figure 9b depicts the identification of a symmetry event that is intrinsic to the trajectory shown.

(As a side note, the boundaries of the symbol tiles are symbol boundaries; thus a symbol tiling represents an event-driven model. It is also possible to create tilings corresponding to time-driven models, but they would amount simply to histograms of the frequency ratio. A discrete-time, time-driven model, would also have to confront the complications of sampling at the "forbidden" state transitions where a trajectory simultaneously crosses symbol tile boundaries in both the vertical and horizontal directions. In the physical world, the effects of temporal race conditions, mechanical non-uniformity, etc. essentially make the "forbidden" state transitions pathological cases.)

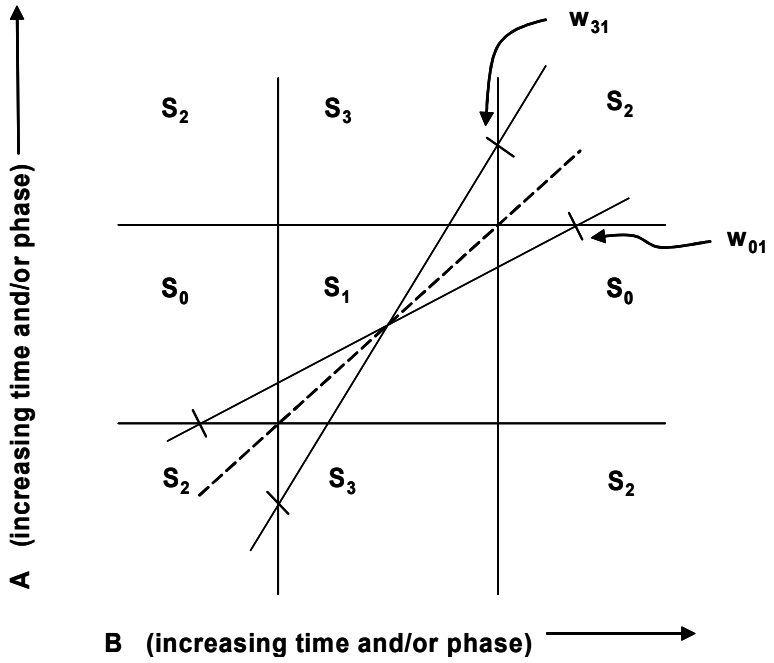

Figure 10

Continuing the study made possible by the infinite periodic quantized-symbol tiling model, Figures 10 and 11 illustrate how varying the slope of a trajectory, which is determined by the ratio of the frequencies of the two oscillators, changes the class of incurred symmetry events. Figure 10 shows a trajectory with slope greater than unity incurring a w_{31} symmetry event, as well as a trajectory with slope less than unity incurring a w_{01} symmetry event. Referring to the table of Figure 3b, the w_{31} symmetry event implies oscillator A is faster than B, while the w_{01} symmetry event implies oscillator B is faster than A, in agreement with the situation depicted in Figure 10.

In general, as the trajectory slope attains values above or below unity, different classes of symmetry events occur. Each of the resulting two symmetry event classes yields a complementary indication as to which oscillator has the higher frequency. As to this, Figure 11 illustrates portions of trajectories associated with each of the eight symmetry events. Referring again to the table of Figure 3b, the four symmetry events w_{02}, w_{13}, w_{20}, w_{31} incurred on trajectories with slopes greater than unity are associated with oscillator A being faster than B, while the four symmetry events w_{01}, w_{10}, w_{23}, w_{32} incurred on trajectories with slopes less than unity are associated with oscillator B being faster than A.

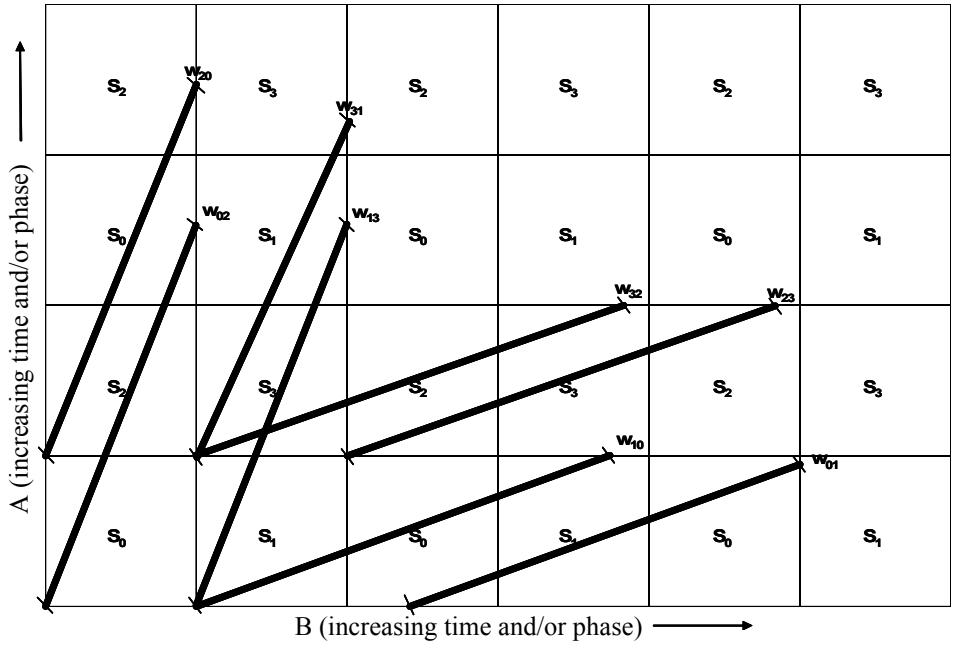

Figure 11

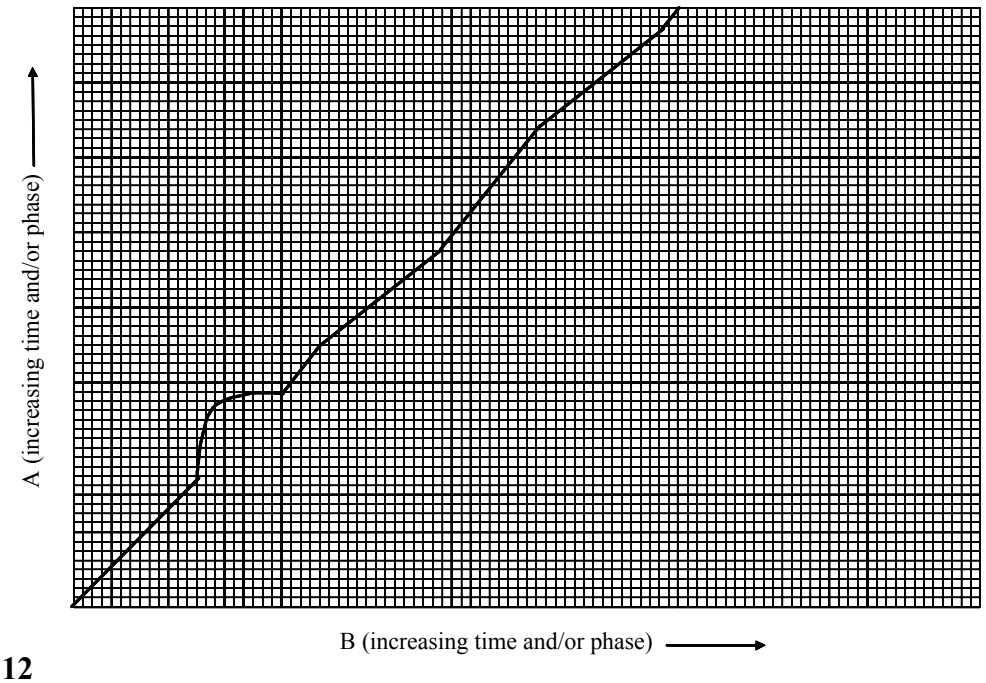

Figure 12

Figure 12 illustrates a view of a portion of a trajectory of a pair of waveforms whose relative ratio of oscillating frequencies varies over time. Note that the scale of the view is considerably larger than in the preceding figures and that each square represents an individual symbol tile, here unmarked for the sake of clarity. Here, the trajectory through the infinite periodic tiling representation changes as the ratio of the frequencies of the two oscillators changes. Several phenomena are depicted. The trajectory first traverses an epoch of time where the two oscillators have a fixed frequency ratio, then an epoch with a meandering ratio, and then an epoch of piecewise-constant periodic modulation. Other frequency-related trajectory phenomena, particularly those pertaining to frequency modulation and phase modulation, can be depicted, noting that frequency modulation is time-differentiated phase modulation while phase modulation is time-integrated frequency modulation.

ASYMMETRIC PULSE WAVES AND THEIR SYMBOLIC DYNAMICS FEATURES

Many common oscillators constructed from feedback loops introduced around logic gates (for example, CMOS inverter gates) produce slightly asymmetric waveforms that differ in duty-cycle from that of complete symmetry (50%) by values such as 3% or more. In practice, all square wave oscillators will produce binary-valued waveforms that are at least slightly asymmetric.

Additionally, when the frequency of a square wave oscillator is modulated, asymmetries in pulse width are introduced as the waveform period expands or contracts. If the frequency is modulated relatively rapidly with respect to the oscillator frequency or with a large modulation index, these asymmetries can be significant. If the frequency is modulated relatively slowly with respect to the oscillator frequency, or with a small modulation index, the asymmetries are insignificant.

When an asymmetric binary-valued pulse waveform is compared to another waveform whose frequency is sufficiently close, a number of additional phenomena can occur:

- the narrower portion of one asymmetric square wave experiences an enveloping event with respect to either:
    - symmetric portions of a fully symmetric ideal square wave, or
    - the wider portion of the other asymmetric square wave;
- the wider portion of one asymmetric square wave experiences an enveloping event with respect to either:
    - symmetric portions of a fully symmetric ideal square wave, or
    - the narrower portion of the other asymmetric square wave.

These additional phenomena can confuse the methods described thus far.

The degree to which these phenomena can occur is bounded by how close the waveforms are in frequency and how asymmetric each of the waveforms is. In cases where the frequencies of two compared waveforms are close enough to create these phenomena, a natural solution for many applications is to employ toggle flip-flops to homogenize the symmetry.

However, various types of asymmetric conditions and the phenomena they induce can be readily detected, and in many cases adverse effects may be readily corrected. This section considers extensions of the invention to handle asymmetric binary-valued pulse waveforms.

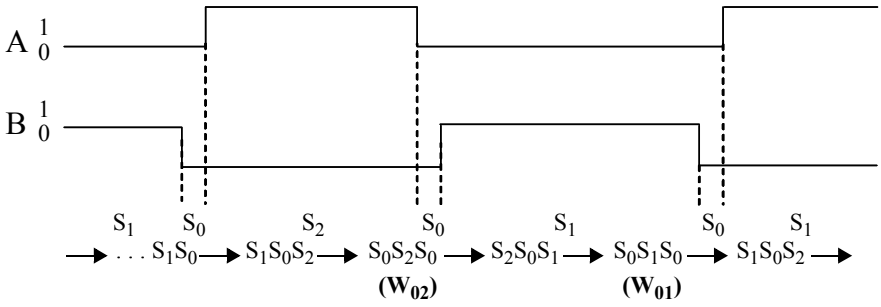

Figure 13a

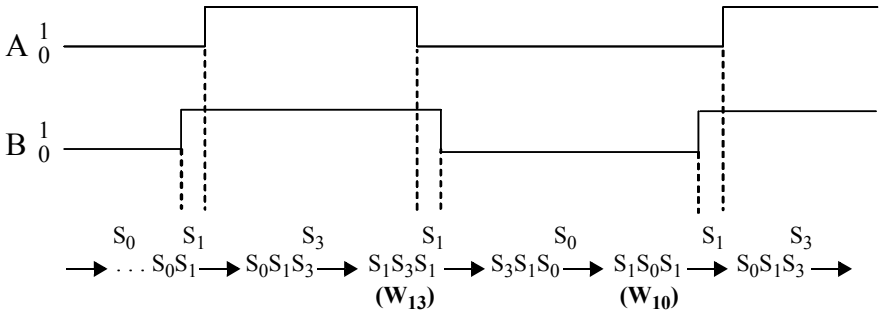

Figure 13a

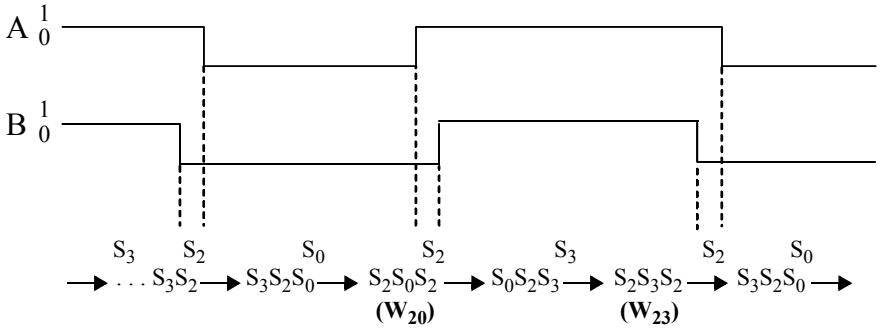

Figure 13a

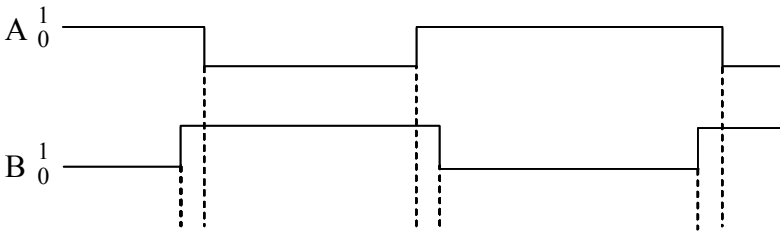

When the input to implementations of the invention designed specifically for symmetric waveforms are asymmetric waveforms, and when the frequencies of the asymmetric waveforms are sufficiently close, alternating indications that each of the waveforms is faster than the other can result. Referring to Figures 13a-d, four cases (polarity combinations) of asymmetric pulse waves of almost the same frequency and almost the same (asymmetric) duty cycle are shown. As may be seen in this figure, under these conditions asymmetric pulse waveforms have unique signature events as well, expressible in terms of "signature" sequences of symmetry events:

- if the enveloping event resulting from the asymmetry involves brief flashes of the S_0 symbol, there will be a sequence of w_{01} and w_{02} symmetry events separated by one non-symmetry event;
- if the enveloping event resulting from the asymmetry involves brief flashes of the S_1 symbol, there will be a sequence of w_{10} and w_{13} symmetry events separated by one non-symmetry event;
- if the enveloping event resulting from the asymmetry involves brief flashes of the S_2 symbol, there will be a sequence of w_{20} and w_{23} symmetry events separated by one non-symmetry event;
- if the enveloping event resulting from the asymmetry involves brief flashes of the S_3 symbol, there will be a sequence of w_{31} and w_{32} symmetry events separated by one non-symmetry event.

Note that the pairs of symmetry events in each list item are complementary in that the first symmetry event implies one oscillator would be faster if its pulse waveform were symmetric while the other symmetry event implies the opposite. Without special considerations, then, these phenomena create problematic alternating indications that each of the oscillators is faster when the frequencies are close enough so that slight asymmetries in the input waveforms are within the measurement capture range of the aforementioned implementations of the invention.

Several additional interesting algebraic relationships are also inherent in the above list of observations. If the frequencies of the two square waves are very close, the sequence will repeat in an alternating pattern for two or more times, and the number of times increases monotonically as the relation between the frequencies approaches identity. Further, each of the conditions in the above list identifies a unique type of relative asymmetry inherent in the pair of waveforms. These facts, and similar ones resulting from other cases (more divergent asymmetry, one waveform essentially symmetric while the other is asymmetric, etc.) may be used to create additional circuitry or algorithms to detect and indicate these events, unique to the asymmetries involved. Additionally, once the asymmetries are detected, the phenomena that would otherwise produce a confused outcome for the circuitry and algorithms can be used to produce definitive frequency comparison outcomes, and even provide additional information about the asymmetries.

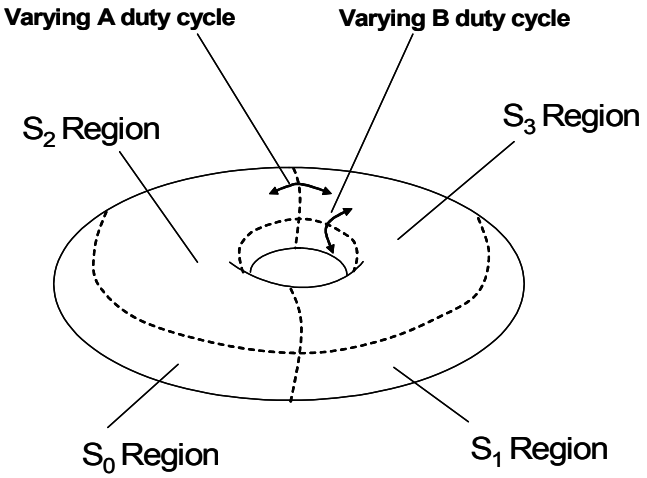

Figure 14

The general background as to the behavior of pairs of asymmetric pulse waveforms can be further rendered in terms of modified versions of the symbolic dynamics models introduced for the symmetric case. Figure 14 illustrates a variation of the symmetrically quantized torus of Figure 8 adapted for use with asymmetric pulse waveforms. Here, the region boundaries determining the quantization thresholds on the continuous-valued, continuous-time oscillator torus surface may be adjusted (as indicated by the arrows) so as to obtain different duty cycles. Clearly, this affects the resulting event-driven symbol sequence.

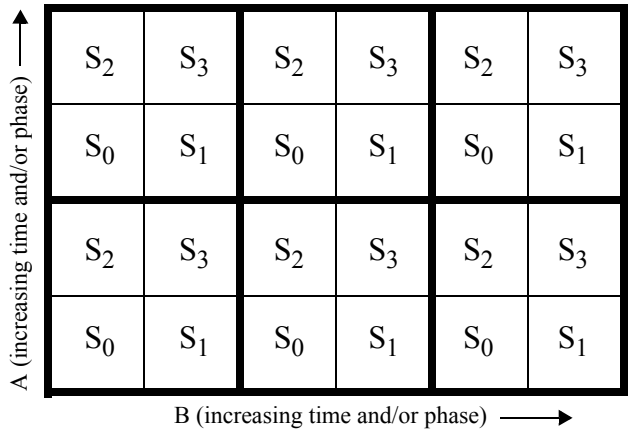

Figure 15a

Further detail can be seen by adapting the infinite periodic quantized-symbol tiling model to asymmetric pulse waveforms. Figure 15a illustrates an asymmetric sequential tiling representation of the asymmetrically quantized torus of Figure 14, akin to the sequential tiling representation shown in Figure 9a of the symmetrically-quantized torus of Figure 8a. As with Figure 9a, each larger tile corresponding to the full torus surface is indicated with a thick line boundary, and each larger tile of the full torus surface is evenly subdivided into four separate areas. These subdivided areas within each of the full torus-surface tiles will be termed "symbol tiles." In the vertical direction, there are two alternating types of columns, one that sequences between S_0 and S_2 symbol tiles and another that sequences be-

tween S_1 and S_3 symbol tiles. In the horizontal direction, there are two alternating types of rows, one that sequences between S_0 and S_1 symbol tiles and another that sequences between S_2 and S_3 symbol tiles.

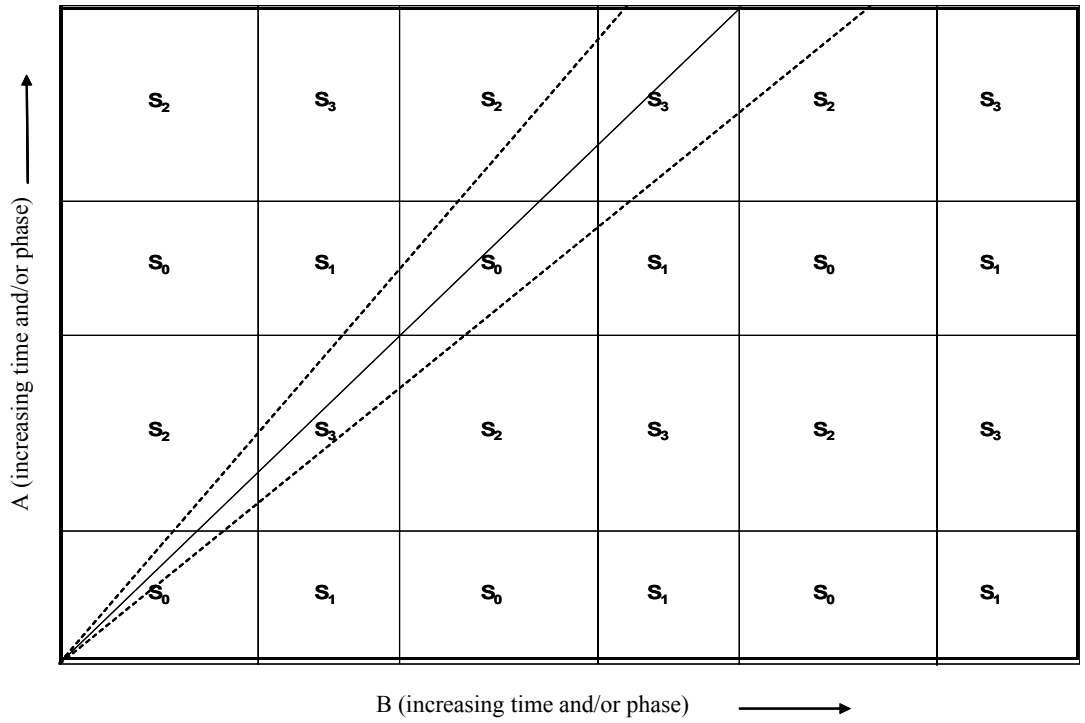

Figure 15b

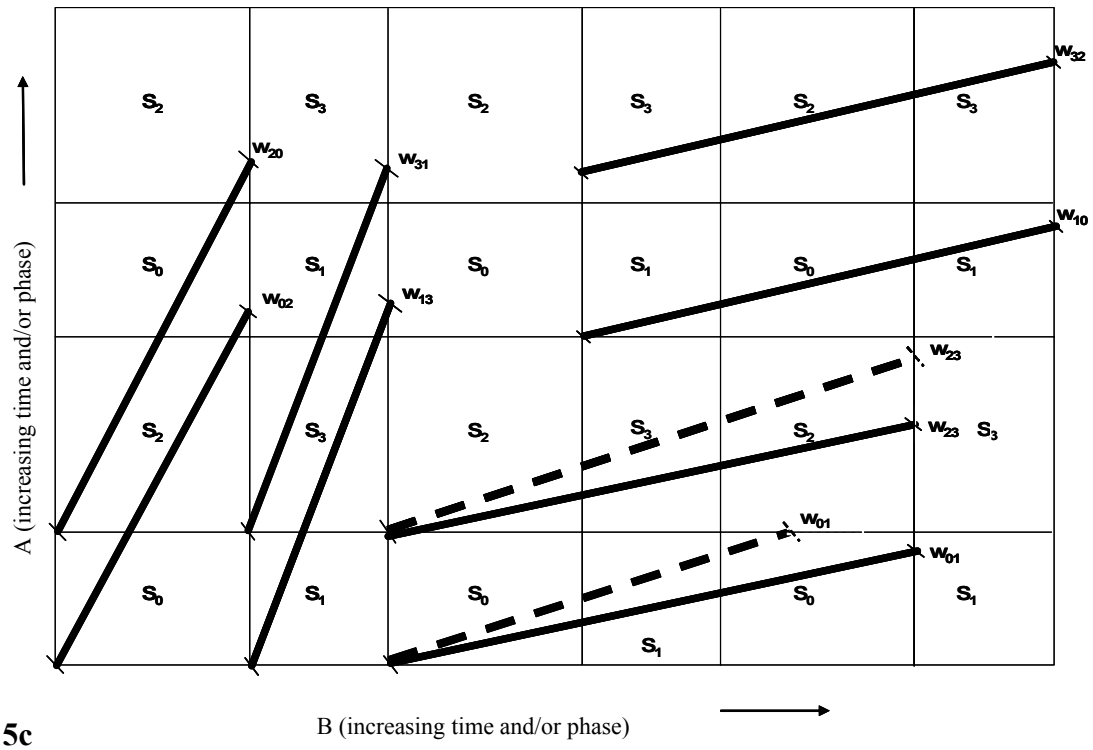

Figure 15c

Figure 15b illustrates three exemplary trajectories associated with fixed frequency ratios of unity, less than unity, and greater than unity, in their traversal over the asymmetric sequential tiling. Using the notions of Figures 15a-b, Figure 15c illustrates portions of sample trajectories associated with each of the eight symmetry events of the invention. Note in particular that the two parallel solid-marked spans of symmetry events w_{23} and w_{01} are of equal length, while at a slightly different frequency ratio the two dashed-marked spans of symmetry events w_{23} and w_{01} are of unequal length as a result of the waveform asymmetry.

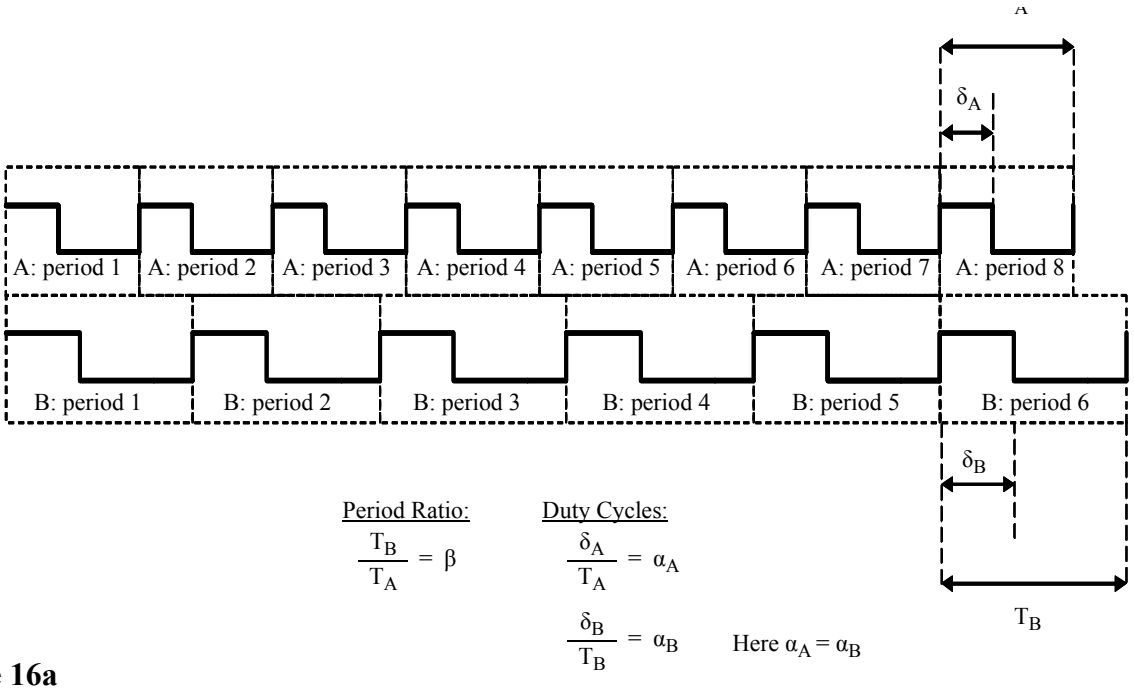

Figure 16a

Attention now is directed to the relation between closeness in frequency and degrees of asymmetry that give rise to asymmetric events and the duration of constituent alternating patterns of complementary event symbols. To begin, Figure 16a illustrates timing notations that may be applied to an exemplary pair of asymmetric input waveforms that share a nearly identical asymmetric duty cycle. The top waveform comprises an asymmetric pulse pattern with a given duty cycle (other than 50%) which repeats periodically at a given rate to form pulse wave A. The lower waveform is a time-stretched version of the original asymmetric pulse pattern. This time-stretched version repeats periodically to form a slower pulse wave B of lower frequency of the same duty-cycle. In this example, the period of the time-stretched version is depicted as 7/5 longer than the period of the original asymmetric pulse pattern. The ratio of frequency of pulse wave A to frequency of pulse wave B is 7/5, and their co-aligned phase-locked pattern repeats every 7 cycles of pulse wave A and every 5 cycles of pulse wave B. (For the predominant cases where one or both of the frequencies either drift from the particular phase-lock condition of Figure 16a or are non-commensurable, the relative positions of the waveforms will shift variably over time.) For subsequent discussion and additional calculation, the following quantities are defined:

- the period of waveform A is T_A, measured in units of time;

- the period of waveform B is T_B, measured in units of time;
- the duty-duration of waveform A is δ_A, measured in units of time;
- the duty-duration of waveform B is δ_B, measured in units of time;
- the duty-cycle of waveform A is α_A, measured as a dimensionless fraction;
- the duty-cycle of waveform B is α_B, measured as a dimensionless fraction;
- the duration over which waveform A has logical value 0 is $T_{(a=0)}$, measured in units of time;
- the duration over which waveform A has logical value 1 is $T_{(a=1)}$, measured in units of time;
- the duration over which waveform B has logical value 0 is $T_{(b=0)}$, measured in units of time;
- the duration over which waveform B has logical value 1 is $T_{(b=1)}$, measured in units of time;
- the period ratio of waveform B to waveform A is $\beta = T_B / T_A$.

Note that δ_A and $T_{(a=1)}$ are equivalent, as are δ_B and $T_{(b=1)}$. Additionally, for the example above, $\beta = 7/5$ and $\alpha_A = \delta_B$. Also, since the period is the reciprocal of the frequency, the ratio of the period of waveform B to the period of waveform A is identical to the ratio of their frequencies, as defined throughout this document.

In a situation in contrast to that of Figure 16a, Figure 16b illustrates a case where the frequency ratio is only a tiny amount larger than 7/5. This frequency ratio guarantees the eventual occurrence of a situation depicted in Figure 16b, where the enveloping occultations (or enveloping) of the asymmetric aspects of two asymmetric waveforms whose frequencies are sufficiently close togethe,r result in alternating indications that each of the oscillators is faster than the other.

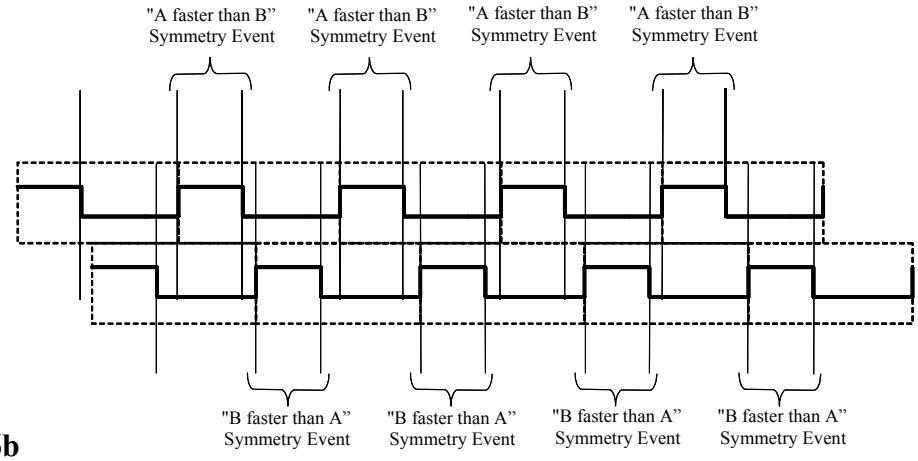

Figure 16b

Taking a slightly larger view, pairs of asymmetric waveforms whose frequencies are sufficiently close exhibit alternating intervals of the behavior associated with symmetric waveforms and intervals of asymmetry events comprising alternating indications of symmetry events (the situation depicted in Figure 16b is an example of the latter) as non-phase-locked waveforms slip by one another. This alternation can be viewed as a type of macro-cycle (although if the frequencies are non-commensurable, this macroscopic behavior will not be periodic but rather slowly evolving). In general, the macroscopic behavior will be like that depicted in Figures 17a-d. In particular, Figures 17a-d call out the four macroscopic behavioral signatures corresponding to each of the four asymmetry events depicted in Figures 13a-d. These four signatures are distinguished by the presence of specific pairs of complementary symmetry events. These signatures indicate relationships that exist among $T_{(a=0)}$, $T_{(a=1)}$, $T_{(b=0)}$, and $T_{(b=1)}$. Note that all of this is simply a formalization of the geometric pulse width relationships depicted in Figures 13a-d.

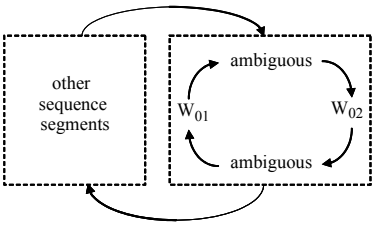

Figure 17a Signature of $\{T_{(a=0)}>T_{(a=1)}, T_{(b=0)}>T_{(b=1)}\}$

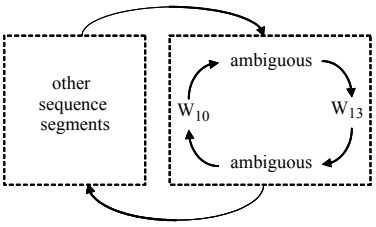

Figure 17b Signature of $\{T_{(a=0)}>T_{(a=1)}, T_{(b=1)}>T_{(b=0)}\}$

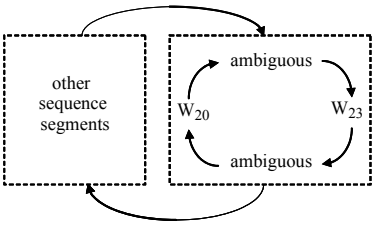

Figure 17c Signature of $\{T_{(a=1}>T_{(a=0)}, T_{(b=0)}>T_{(b=1)}\}$

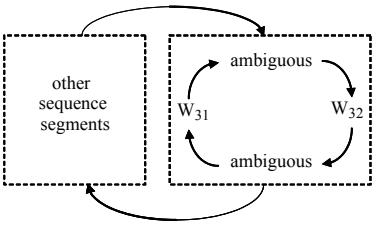

Figure 17d Signature of $\{T_{(a=1}>T_{(a=0)}, T_{(b=1)}>T_{(b=0)}\}$

In a more general view of the macro-cycles depicted in Figures 17a-d, Figures 18a-c depict the evolution of macro-cycle behavior that occurs for waveforms with (even minor) asymmetry as the frequency ratio is increased from a value sufficiently lower than unity, through ratios sufficiently close to unity, and then to ratios sufficiently greater than unity. Figure 19a illustrates the macro-cycle behavior for the case where the frequency ratio is a value sufficiently lower than unity. Figure 19b illustrates the case where the frequency ratio is close enough to unity that the waveform asymmetry (however small it may be) becomes theoretically detectable. However, in any physical implementation, the minimum response times of the logic circuitry, mechanical apparatus, chemical process, sampling rate for data provided to algorithmic implementations, etc. will determine a minimum threshold for detecting this situation. As the frequency ratio continues to increase to ratios sufficiently greater than unity, the behavior will become that depicted in Figure 19c.

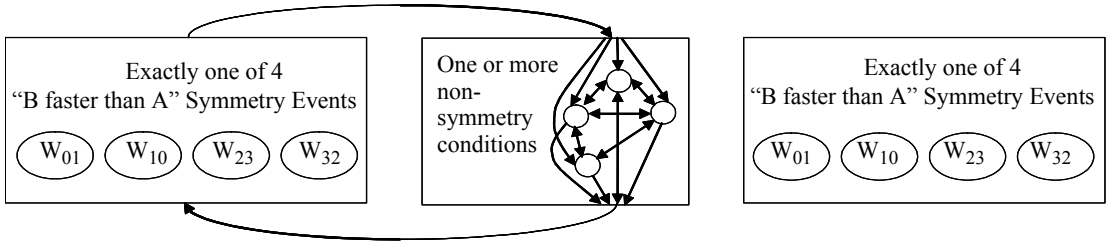

Figure 18a

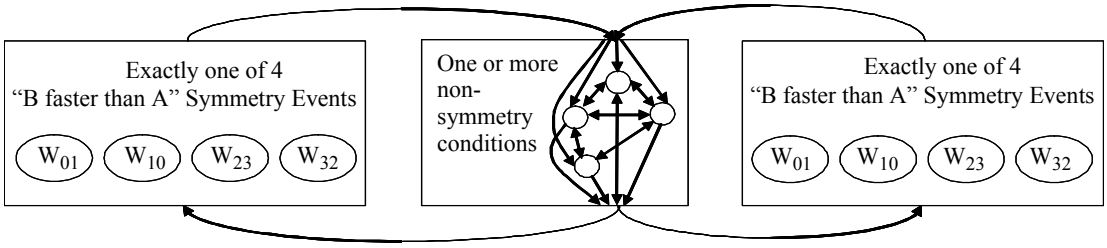

Figure 18b

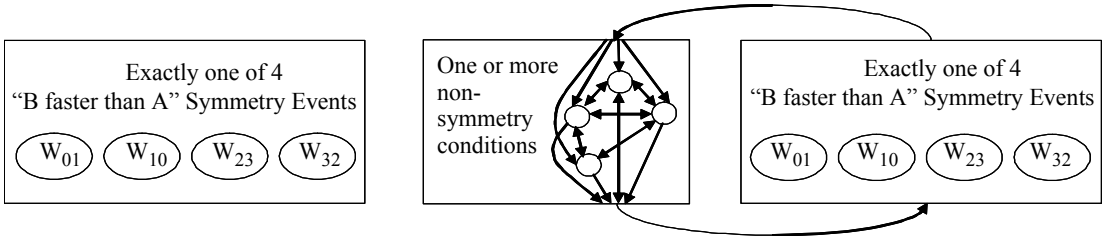

Figure 18c

The phenomena depicted in Figure 19b may be understood in terms of the example of Figures 18a-c. For two waveforms whose frequencies are close together, one of the waveforms may be viewed as progressing past the viewpoint of the other waveform. The rate of this progression is proportional to the difference in frequencies (and so is similar to a "beat frequency," well known in the fields of vibrational mechanics, acoustics, and communications). As one waveform progresses past the other, the waveform asymmetries exhibit various occultations of one another. In particular, Figures 19a-c illustrate the evolution of symbol sequences and symmetry events before, during, and after occultations of asymmetric aspects of two exemplary asymmetric input waveforms with frequencies sufficiently close together. Before occultation, there are no symmetry events, as illustrated in Figure 19a. During occultation, the asymmetric aspects give rise to various asymmetry events, in particular, the sequence of complementary symmetry events w_{02}, w_{01}, w_{02} and w_{01}, as illustrated in Figure 19b, which depicts a slight shift in the epoch shown in Figure 19a. After occultation, the asymmetric aspects no longer give rise to asymmetry events, and the situation returns to one like that shown in Figure 19a. This is illustrated in Figure 19c, which depicts a further shift in the epoch shown in Figure 19a.

Formulas may be computed, in terms of the quantities defined earlier, for the upper and lower thresholds at which, for a given frequency ratio and given duty cycles, the behavior

of Figure 19b will begin to appear. These formulas can be extended to characterize other behavior (depicted in Figures 17a-d), such as the temporal duration of macro-cycles, the number of alternations of complementary symmetry events in a macro-cycle, the frequency of these alternations, etc. Threshold formulas may be further adjusted to account for minimum response times, sampling rates, and other factors, to determine a minimum threshold for which asymmetry situations can be detected. Such formulas may be used to characterize the limitations of a particular embodiment. Additionally, they may be used to design or create additional features, capabilities, and extensions. For example, the use of resettable counters in conjunction with detection of specific alternating complementary symmetry events may be used to further characterize waveform asymmetries and specific aspects of asymmetry events that may be useful in specific applications.

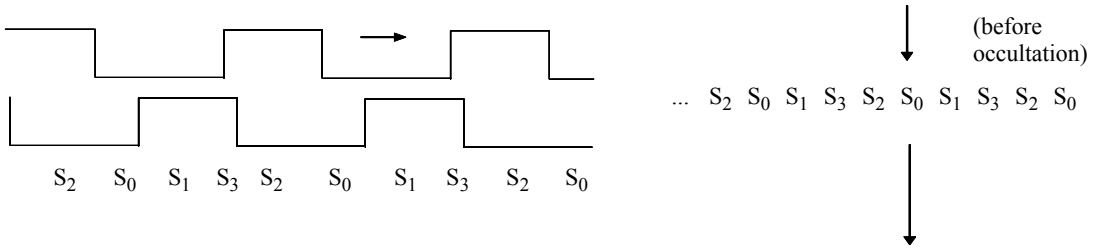

Figure 19a

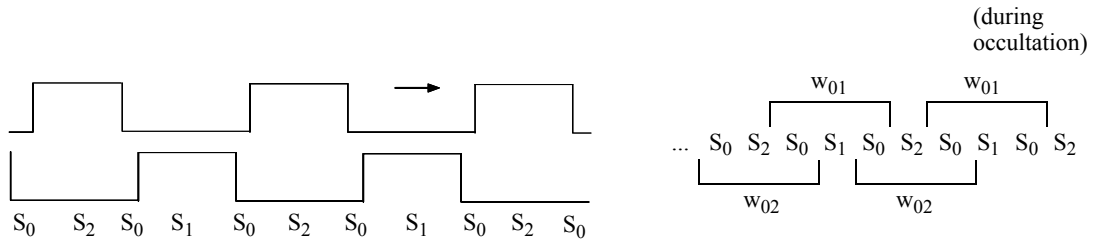

Figure 19a

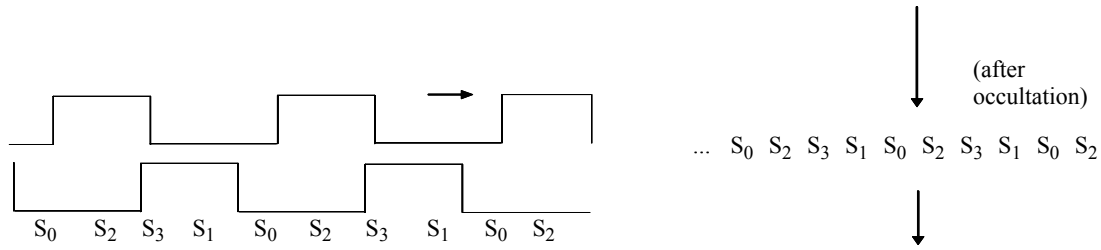

Figure 19c

REFERENCES

[1] Bai-Lin, Hao, Elementary Symbolic Dynamics and Chaos in Dissipative Systems, World Scientific, Singapore 1989, ISBN 9971-50-682-3.

[2] Hale, Jack K.; Kocak, Huseyin, Dynamics and Bifurcations, Springer-Verlag, New York, 1991, ISBN 0-387-97141-6.

[3] Kitchens, Bruce P., Symbolic Dynamics - One-sided, Two-sided and Countable State Markov Shifts, Springer-Verlag, Berlin 1998, ISBN 3-540-62738-3.

[4] Nerurkar, M. G.; Dokken, D. P.; Ellis, D. B. (eds.), Topological Dynamics and Applications, *Contemporary Mathematics*, American Mathematical Society, Providence.

[5] Walters, Peter (ed.), Symbolic Dynamics and its Applications, *Contemporary Mathematics*, American Mathematical Society, Rhode Island 1992, ISBN 0-8218-5146-2.

[6] Williams, Susan G. (ed.), Symbolic Dynamics and its Applications, *Proceedings of Symposia in Applied Mathematics*, American Mathematical Society, Providence 2004, ISBN 0-8218-3157-7.